

Synthesis and Comparative *In Vivo* Evaluation of Site-Specifically Labeled Radioimmunoconjugates for DLL3-Targeted ImmunoPET

Sai Kiran Sharma, Pierre Adumeau, Outi Keinänen, Vikram Sisodiya, Hetal Sarvaiya, Robert Tchelepi, Joshua A Korsen, Jacob Pourat, Kimberly J. Edwards, Ashwin Ragupathi, Omar Hamdy, Laura R. Saunders, Charles M. Rudin, John T. Poirier, Jason S. Lewis, and Brian M. Zeglis*

Cite This: *Bioconjugate Chem.* 2021, 32, 1255–1262

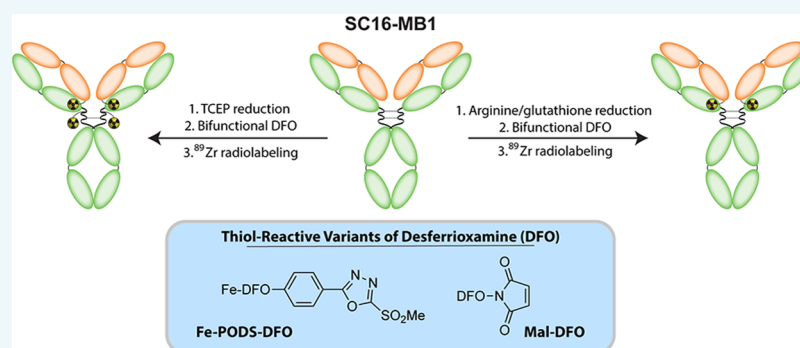
Read Online

ACCESS |

Metrics & More

Article Recommendations

Supporting Information



ABSTRACT: Delta-like ligand 3 (DLL3) is a therapeutic target for the treatment of small cell lung cancer, neuroendocrine prostate cancer, and isocitrate dehydrogenase mutant glioma. In the clinic, DLL3-targeted ^{89}Zr -immunoPET has the potential to aid in the assessment of disease burden and facilitate the selection of patients suitable for therapies that target the antigen. The overwhelming majority of ^{89}Zr -labeled radioimmunoconjugates are synthesized via the random conjugation of desferrioxamine (DFO) to lysine residues within the immunoglobulin. While this approach is admittedly facile, it can produce heterogeneous constructs with suboptimal *in vitro* and *in vivo* behavior. In an effort to circumvent these issues, we report the development and preclinical evaluation of site-specifically labeled radioimmunoconjugates for DLL3-targeted immunoPET. To this end, we modified a cysteine-engineered variant of the DLL3-targeting antibody SC16-MB1 with two thiol-reactive variants of DFO: one bearing a maleimide moiety (Mal-DFO) and the other containing a phenyloxadiazolyl methyl sulfone group (PODS-DFO). In an effort to obtain immunoconjugates with a DFO-to-antibody ratio (DAR) of 2, we explored both the reduction of the antibody with tris(2-carboxyethyl) phosphine (TCEP) as well as the use of a combination of glutathione and arginine as reducing and stabilizing agents, respectively. While exerting control over the DAR of the immunoconjugate proved cumbersome using TCEP, the use of glutathione and arginine enabled the selective reduction of the engineered cysteines and thus the formation of homogeneous immunoconjugates. A head-to-head comparison of the resulting ^{89}Zr -radioimmunoconjugates in mice bearing DLL3-expressing H82 xenografts revealed no significant differences in tumoral uptake and showed comparable radioactivity concentrations in most healthy nontarget organs. However, ^{89}Zr -DFO_{PODS}-^{DAR2}SC16-MB1 produced 30% lower uptake (3.3 ± 0.5 %ID/g) in the kidneys compared to ^{89}Zr -DFO_{Mal}-^{DAR2}SC16-MB1 (4.7 ± 0.5 %ID/g). In addition, H82-bearing mice injected with a ^{89}Zr -labeled isotype-control radioimmunoconjugate synthesized using PODS exhibited ~40% lower radioactivity in the kidneys compared to mice administered its maleimide-based counterpart. Taken together, these results demonstrate the improved *in vivo* performance of the PODS-based radioimmunoconjugate and suggest that a stable, well-defined DAR2 radiopharmaceutical may be suitable for the clinical immunoPET of DLL3-expressing cancers.

The rapid rise of monoclonal antibodies as platforms for molecularly targeted diagnostics and therapeutics has necessitated a parallel surge in the development of bioconjugation methods.¹ Historically, the modification of antibodies has been achieved via the random ligation of amine-reactive cargoes—toxins, fluorophores, radionuclides, *etc.*—with lysine residues of the biomolecule.² This approach is unquestionably simple and straightforward, though it is not

Special Issue: State-of-the-Art of Radiometal-based Bioconjugates for Molecular Imaging and Radiotherapy

Received: March 10, 2021

Published: April 9, 2021



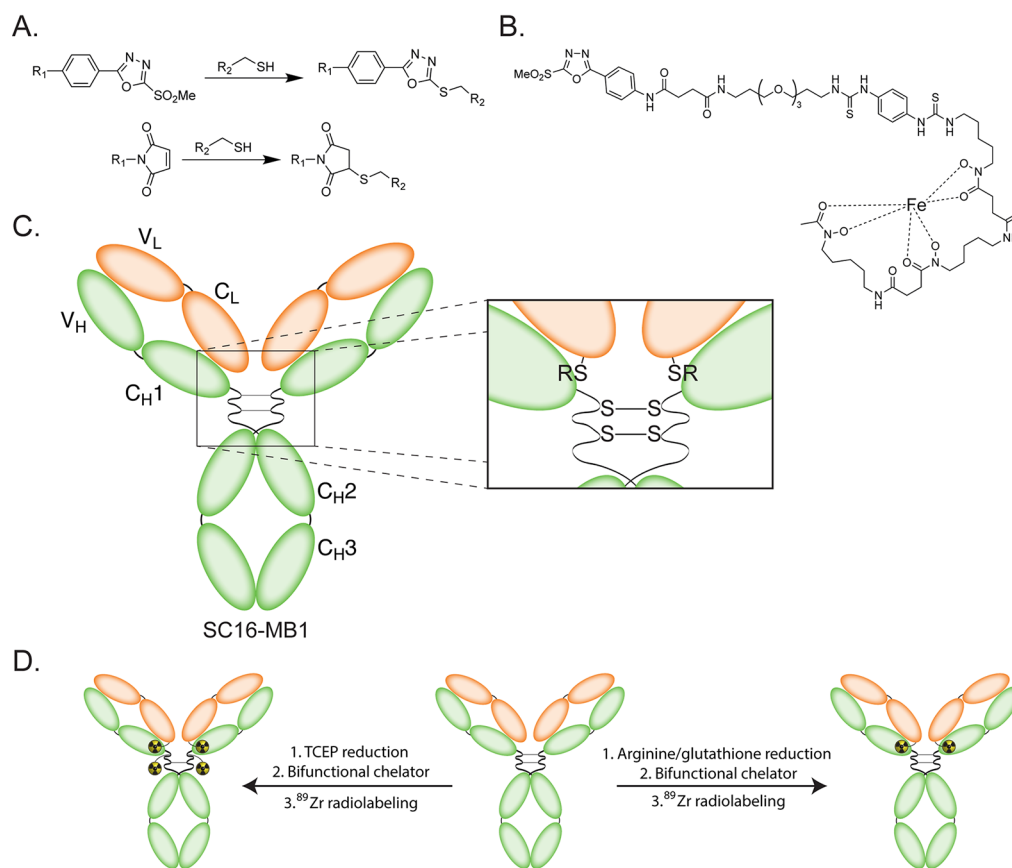


Figure 1. (A) Schematic of the ligations between PODS (top) and a maleimide (bottom) with a thiol moiety; (B) structure of PODS-DFO-Fe; (C) schematic of SC16-MB1 with inset illustrating the position of the native interchain disulfide bridges as well as the genetically engineered capped thiol residues (-SR) within the light chain; (D) generalized schematic of the bioconjugation results obtained using the different approaches to reduction described in this work.

without its costs: stochastic bioconjugation strategies have been repeatedly shown to create poorly defined and heterogeneous immunoconjugates with suboptimal *in vitro* and *in vivo* performance.¹ In response to this issue, a wide variety of site-specific bioconjugation strategies have been developed, including variants based on unnatural amino acids, glycoengineering, and chemoenzymatic transformations.^{3–8}

The most facile and common strategies for the site-specific bioconjugation of antibodies rely on ligations between thiol-reactive probes and the cysteine residues that form the biomolecule's interchain disulfide bonds.^{5,6} The recent advent of engineered immunoglobulins that contain *free* cysteines has further bolstered the utility of these approaches.^{3,9} Maleimides are easily the most commonly used prosthetic groups for cysteine-based conjugations (Figure 1A). Yet, their popularity stands in stark contrast to persistent concerns regarding the *in vivo* stability of their linkage with thiols.^{10–15} The succinimidyl thioether bond formed between maleimides and thiols has been shown to be susceptible to retro-Michael reactions *in vivo*, a process that can result in the release of the payload or its exchange with other thiol-containing biomolecules. This is an especially problematic phenomenon for radioimmunoconjugates, because the *in vivo* release of radiometals—or, for that matter, radiometal–chelator complexes—can increase radioactivity concentrations in healthy, nontarget tissues. In the context of nuclear imaging, this can decrease tumor-to-background contrast; in the context of radioimmunotherapy, this can increase radiation dose rates to healthy tissues and

thus reduce therapeutic indices. A variety of alternative thiol-reactive prosthetic groups have been developed in an effort to mitigate these drawbacks, including tosylates, halo-acetyls, vinyl sulfones, and “second generation” maleimides capable of hydrolyzing to more stable structures.^{14,16–22} Yet, each of these new additions to the bioconjugation toolbox brings with it a new set of limitations, including sluggish reactivity and a lack of specificity for thiols.

In this investigation, we have harnessed an emergent, thiol-reactive bioconjugation reagent based on a phenyloxadiazolyl methyl sulfone (PODS) core to create a site-specifically modified ⁸⁹Zr-radioimmunoconjugate as a companion diagnostic for a DLL3-targeted antibody–drug conjugate (ADC). PODS-based reagents react quickly, cleanly, and (unlike maleimides) irreversibly with thiols (Figure 1A).^{23–27} Even more importantly, we have previously demonstrated that the site-selective modification of wild-type antibodies with PODS-bearing chelators produces ¹⁷⁷Lu- and ⁸⁹Zr-labeled radioimmunoconjugates with high stability and excellent *in vivo* performance (Figure 1B).²³

The centerpiece of this investigation is SC16-MB1, a humanized antibody that targets DLL3—a tumor antigen expressed in small cell lung cancer, neuroendocrine prostate cancer, and isocitrate dehydrogenase mutant glioma—and forms the basis for an ADC (rovalpituzumab teserine) that has shown therapeutic efficacy in murine models of SCLC.^{28–30} Importantly, SC16-MB1 has been genetically engineered to contain two free cysteine residues that facilitate the attachment

Table 1. Description of the Bioconjugation Results for the SC16-MB1 and hIgG1-MB1 Immunoconjugates^a

immunoconjugate	free thiols	average DAR	fraction of constructs with DFO-to-mAb ratio (DAR)						
			0	1	2	3	4	5	6
DFO _{Mal} ^{TCEP^{low}} SC16-MB1	1.2 ± 0.2	0.85	57.4	1.0	40.5	1.1	0.0	0.0	0.0
DFO _{Mal} ^{TCEP^{high}} SC16-MB1	3.4 ± 0.1	3.41	5.6	0.9	39.2	1.7	28.6	1.5	22.51
DFO _{Mal} ^{DAR²} SC16-MB1	1.9 ± 0.0 ⁴	1.81	13.9	1.0	76.1	1.6	6.0	0.0	1.5
DFO _{PODS} ^{DAR²} SC16-MB1	1.4 ± 0.0 ³	1.00	30.6	38.2	31.2	0.0	0.0	0.0	0.0
DFO _{Mal} ^{DAR²} hIgG1-MB1	1.8 ± 0.1	1.73	17.7	0.0	78.1	0.0	4.2	0.0	0.0
DFO _{PODS} ^{DAR²} hIgG1-MB1	1.3 ± 0.1	1.26	22.6	28.7	48.7	0.0	0.0	0.0	0.0

^aThe number of free thiols prior to bioconjugation was determined using Ellman's reagent. The average DFO-to-mAb ratio (DAR) and the fraction of constructs with each individual DAR were determined via mass spectrometry.

of thiol-reactive probes. SC16-MB1—like wild-type IgG1—contains a pair of interchain disulfides that bridge the heavy chains of the lower hinge region (Figure 1C). In the upper hinge region, however, the heavy chain cysteines that would normally form disulfide links with the light chain have been mutated, leaving a pair of capped free cysteines on the light chain that are available for bioconjugation. Herein, we describe the synthesis, chemical characterization, and *in vitro* evaluation of site-specifically modified immunoconjugates of SC16-MB1 using maleimide- and PODS-bearing variants of desferrioxamine (DFO), the current “gold standard” chelator for zirconium-89.³¹ As part of our methodology development, two different reduction strategies were employed in order to ensure the modification of the pair of genetically engineered free cysteines *without* altering the immunoglobulin's disulfide bridges (Figure 1D). Subsequently, we employed a series of these ⁸⁹Zr-labeled radioimmunoconjugates for PET imaging and biodistribution experiments in a subcutaneous xenograft model of SCLC to determine if the contrasting approaches to bioconjugation manifested in differences in the *in vivo* performance of the two radioimmunoconjugates. Ultimately, it is our hope that this work leads to the translation of a companion theranostic imaging agent based on SC16-MB1 that could help clinicians select patients that are likely to respond to DLL3-targeted therapies.

RESULTS AND DISCUSSION

Optimizing the Thiol-Mediated Bioconjugations. The relative scarcity of cysteines in immunoglobulins and the nucleophilicity of their sulfhydryl side chains combine to make them singularly useful handles for bioconjugation. The emergence of genetically engineered immunoglobulins that contain free cysteine residues only renders thiol-based bioconjugation approaches *more* attractive.⁶ Importantly, however, two variables must be carefully considered during the construction of any thiol-modified bioconjugate: (1) the reduction conditions used to expose free sulfhydryl groups and (2) the thiol-reactive prosthetic group responsible for attaching the cargo to the biomolecule. We have worked to optimize both during our development of ⁸⁹Zr-DFO-labeled variants of SC16-MB1.

We started our investigation by exploring a pair of strategies designed to expose free sulfhydryl groups on the antibody. The first used TCEP as a mild reducing agent capable of cleaving the antibody's interchain disulfide bridges *and* exposing its genetically incorporated free cysteines.³² The second strategy, in contrast, employed a two-component buffer composed of glutathione (a mild reducing agent) and arginine (a stabilizing agent) that is formulated to selectively reduce the capped free

cysteines in the upper hinge region while leaving the native interchain disulfides untouched.

To begin with the former, our results demonstrate that using 4 mol equiv of TCEP in conjunction with a maleimide-bearing variant of DFO (Mal-DFO) produced an immunoconjugate (DFO_{Mal}^{TCEP^{low}}SC16-MB1) with an average DAR of 0.85. Mass spectrometry revealed that 43% of this immunoconjugate had a DAR ≥ 2, while ~57% remained completely unmodified (Table 1). The continued presence of the parent antibody as well as the apparent absence of modifications to the heavy chain (Figure S1) suggest that this approach to bioconjugation primarily modifies the free cysteines yet fails to uncap these residues completely. Using 10 mol equiv of TCEP, on the other hand, yields an immunoconjugate (DFO_{Mal}^{TCEP^{high}}SC16-MB1) with an average DAR of 3.4 and a wide distribution of species bearing 1–6 chelators per antibody. Specifically, this approach yielded a mixture of species including 39% with a DAR of 2, 28% with a DAR of 4, and 22% with a DAR of 6 (Table 1). This distribution plainly suggests that all 6 thiols were available for bioconjugation to some extent, a notion confirmed by mass spectra illustrating the modification of both light chain (LC) and heavy chain (HC) (Figure S2). In both the TCEP^{low} and TCEP^{high} cases, the average DAR values of the immunoconjugates were in close agreement with the number of free thiols present in the reduced antibody as determined using Ellman's reagent, a result which reinforces the value of this assay for predicting the DAR of immunoconjugates formed via the ligation of free thiols (Table 1). Ultimately, these results suggest that neither set of TCEP-mediated conditions produced an optimal immunoconjugate, but the careful titration of TCEP could be used to ensure the selective reduction of the capped free cysteines without interfering with the disulfides of the lower hinge region.

In an effort to improve the selectivity and completeness of the reduction reaction, we next turned to a two-step procedure that employs a pair of buffers: one for reduction and another for bioconjugation. While the conjugation buffer is a TRIS- and EDTA-containing solution that minimizes reactions with primary and tertiary amines, it is the reduction buffer that is central to achieving the selective modification of the engineered cysteines within SC16-MB1. The ability to uncap these free cysteines while leaving the native disulfides untouched is predicated on the fact that the disulfides—and, by extension, cysteines—of the upper hinge region have been shown to be more susceptible to reduction than the disulfides of the lower hinge region.³² The reduction buffer contains reduced glutathione and arginine, both common laboratory reagents used for the refolding of recombinant proteins. In this recipe, glutathione serves as a mild reducing agent to uncap the

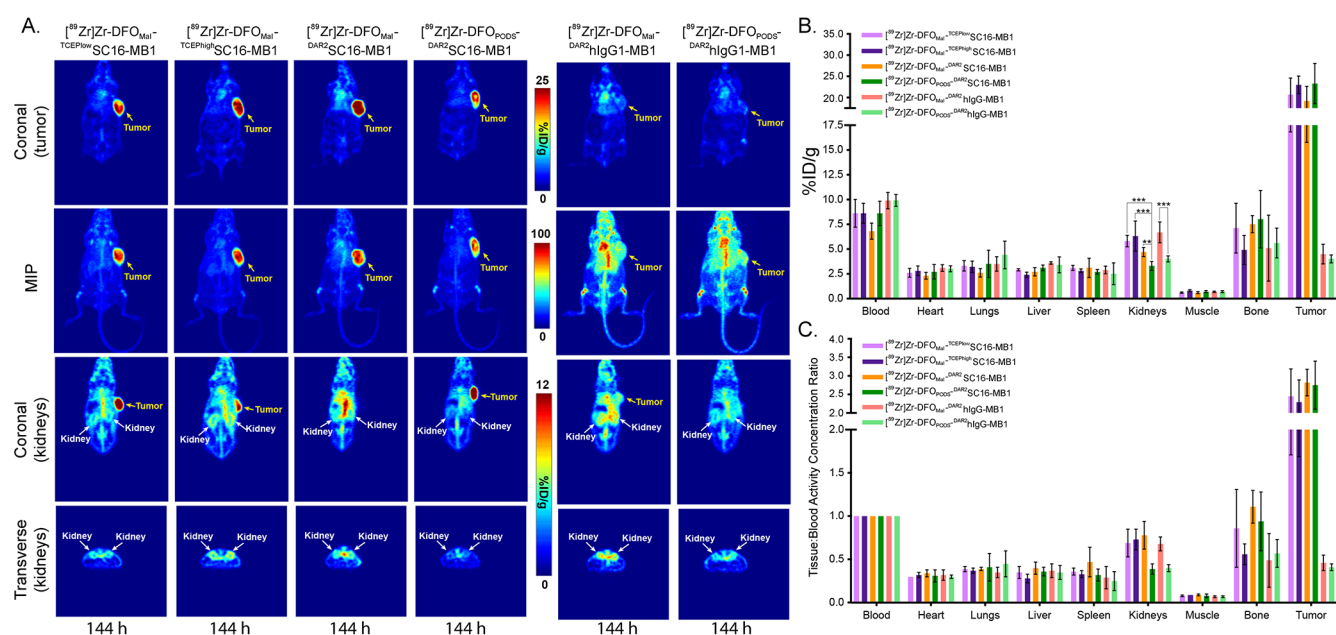


Figure 2. (A) ^{89}Zr -immunoPET images of athymic nude mice bearing DLL3-expressing H82 xenografts acquired at 120–128 h after the administration of $\sim 140\ \mu\text{Ci}$ (1.3 mg/kg) of the SC16-MB1- and hIgG-MB1-based radioimmunoconjugates in 200 μL PBS via the lateral tail vein. The top 2 sets of panels—“coronal (tumor)” and “MIP”—show comparable tumoral uptake between the ^{89}Zr -labeled variants of SC16-MB1, as well as the lower tumoral accretion of the pair of isotype-control radioimmunoconjugates. The bottom 2 panels—“coronal (kidneys)” and “transverse (kidneys)” —reveal that the radioimmunoconjugates synthesized using PODS produce lower radioactivity concentrations in the kidneys. (B) *Ex vivo* biodistribution profiles and (C) tissue-to-blood radioactivity concentration ratios (TBR) as determined 120–128 h p.i. after the administration of $\sim 27\ \mu\text{Ci}$ (0.2 mg/kg) of the SC16-MB1- and hIgG-MB1-based radioimmunoconjugates in 200 μL PBS via the lateral tail vein. The graphs show high tumoral uptake (%ID/g) and TBRs for the SC16-MB1-based radioimmunoconjugates but low uptake for the isotype-control radioimmunoconjugates. The radioimmunoconjugates synthesized using PODS produced lower radioactivity concentrations in the kidneys compared to the analogues created using maleimides. ** indicates $p < 0.005$; *** indicates $p < 0.0005$. A complete list of %ID/g values can be found in Tables S1 and S2.

free cysteines at position 214 of the light chain of the upper hinge region, whereas arginine acts as a stabilizing agent.³³

We first explored this methodology—referred to as the “DAR2” method—alongside Mal-DFO for the site-specific modification of SC16-MB1 as well as a nonspecific isotype-control antibody, hIgG1-MB1. MALDI-ToF mass spectrometry revealed that this approach provided a pair of immunoconjugates— $\text{DFO}_{\text{Mal}}^{\text{DAR}2}\text{SC16-MB1}$ and $\text{DFO}_{\text{Mal}}^{\text{DAR}2}\text{hIgG1-MB1}$ —composed of 15–17% unmodified antibody, 0–1% constructs with DAR of 1, 76–78% constructs with DAR of 2, and 4–9% constructs with DAR greater than 2 (Table 1). This relatively homogeneous profile stands in stark contrast to those produced by the $\text{TCEP}^{\text{high}}$ or TCEP^{low} methods that yielded mixtures including >50% of constructs with a DAR of >2 and >50% of immunoconjugates with a DAR of 0, respectively. Furthermore, the mass spectrometry data indicate that this DAR2 approach predominately results in the attachment of DFO to the LC of the engineered antibodies, confirming that the increased selectivity of this method yields better-defined immunoconjugates (Figure S2). Another important advantage of the DAR2 method relative to the TCEP-based approaches is that the former abrogates the need for optimization, as both arginine and glutathione exist in a vast excess relative to the mAb or bifunctional chelator.

The use of Mal-DFO with a more selective approach to reduction clearly increases the homogeneity of the DFO-bearing immunoconjugates. It does not, however, do anything to allay concerns about the instability of the maleimide–thiol linkage. In order to address this issue, we next performed

bioconjugations using a phenyloxadiazolyl methylsulfone-bearing variant of DFO, PODS-DFO-Fe.²³ More specifically, the DAR2 bioconjugation method was used to append PODS-DFO-Fe to both SC16-MB1 and hIgG1-MB1, producing a pair of immunoconjugates: $\text{DFO}_{\text{PODS}}^{\text{DAR}2}\text{SC16-MB1}$ and $\text{DFO}_{\text{PODS}}^{\text{DAR}2}\text{hIgG1-MB1}$ (Table 1). Both constructs had favorable conjugation profiles—68–78% of immunoconjugates with a DAR of 1 or 2 and virtually no immunoconjugates with DAR >2—yielding an average DAR of ~ 1 . The compositional differences between the maleimide- and PODS-based immunoconjugates—*i.e.*, a significantly lower proportion of constructs with a DAR of 2 for the latter—may be attributable to differences in the reactivity of the two bifunctional chelators in the two-component reaction buffer. This hypothesis is supported by the increased prevalence of HC modifications in the immunoconjugates synthesized using PODS-DFO-Fe compared to those created using Mal-DFO (Figures S3 and S4).

Contrasting the *In Vivo* Performance of the ^{89}Zr -Labeled Radioimmunoconjugates. We next sought to evaluate the *in vivo* behavior of the six immunoconjugates in mice bearing DLL3-expressing H82 xenografts. To this end, each of the immunoconjugates— $\text{DFO}_{\text{Mal}}^{\text{TCEP}^{\text{high}}}\text{SC16-MB1}$, $\text{DFO}_{\text{Mal}}^{\text{TCEP}^{\text{low}}}\text{SC16-MB1}$, $\text{DFO}_{\text{Mal}}^{\text{DAR}2}\text{SC16-MB1}$, $\text{DFO}_{\text{PODS}}^{\text{DAR}2}\text{SC16-MB1}$, $\text{DFO}_{\text{Mal}}^{\text{DAR}2}\text{hIgG1-MB1}$, and $\text{DFO}_{\text{PODS}}^{\text{DAR}2}\text{hIgG1-MB1}$ —were radiolabeled with ^{89}Zr , characterized *in vitro* using radiochemical assays, and evaluated *in vivo* via PET imaging and *ex vivo* biodistribution analysis. Importantly, slight differences in the DAR of the six

immunoconjugates did not impact the radiolabeling of the corresponding ^{89}Zr -labeled immunoconjugates: comparable and consistent specific activities of 4.3–5.0 mCi/mg were obtained in each case ($n = 3$). An ITLC-based serum stability assay revealed slight differences in the stability of the various ^{89}Zr -labeled radioimmunoconjugates. Among the six radioimmunoconjugates, ^{89}Zr -DFO_{Mal}-TCEP^{low}SC16-MB1 exhibited the greatest degree of demetalation after 144 h at 37 °C, but no clear trends were apparent (Figure S5).

In the initial *in vivo* study, PET imaging and biodistribution experiments were conducted with each of the ^{89}Zr -labeled radioimmunoconjugates at a single time point (120 h p.i.) in mice bearing DLL3-expressing H82 small cell lung cancer xenografts. To this end, mice were injected with 1.3 mg/kg of each radioimmunoconjugate for PET imaging ($n = 3$ per radioimmunoconjugate) and 0.2 mg/kg for *ex vivo* biodistribution studies ($n = 5$ per radioimmunoconjugate). The data revealed that the quartet of ^{89}Zr -labeled SC16-MB1 radioimmunoconjugates create comparable and high radioactivity concentrations in the DLL3-positive H82 tumors, with uptake values that range from 19.2 ± 3.5 to 23.3 ± 4.8 %ID/g at 120 h p.i. and are consistent with our previous work employing non-site-specifically modified DLL3-targeting radioimmunoconjugates (Figure 2). As expected, the isotype-control radioimmunoconjugates—*i.e.*, ^{89}Zr -DFO_{Mal}-DAR2hIgG1-MB1 and ^{89}Zr -DFO_{PODS}-DAR2hIgG1-MB1—produced values of <5 %ID/g in the H82 tumors at the same time point. The blood was the compartment with the highest radioactivity concentrations for the isotype-control radioimmunoconjugates and the second highest radioactivity concentrations for the four DLL3-targeted radioimmunoconjugates. This is expected for the hIgG1-MB1-based constructs due to the lack of a target sink. However, we have also previously observed relatively high radioactivity concentrations (up to 8% ID/g) in the blood of H82 xenograft-bearing mice injected with the ^{89}Zr -labeled radioimmunoconjugates of SC16 and imaged at the same time point.²⁸ It is most likely that this phenomenon can be attributed to the relatively low abundance and heterogeneous expression of DLL3 compared to other cancer antigens. Strictly speaking, it cannot be ruled out that a fraction of this radioactivity in the blood may result from retro-Michael additions that prompt the release or migration of ^{89}Zr -DFO-Mal species from the radioimmunoconjugates.^{10,13} If this were the case, however, we would expect larger differences between the radioactivity concentrations in the blood created by the maleimide-bearing radioimmunoconjugates (which are susceptible to this reaction) and their PODS-bearing cousins (which are not). Most of the other nontarget tissues of the animals injected with the six radioimmunoconjugates—except for the bones and kidneys—showed radioactivity concentrations of <6 %ID/g at 120 h p.i. The elevated bone uptake is likely a byproduct of the *in vivo* release of the osteophilic ^{89}Zr -Zr⁴⁺ from the radioimmunoconjugates, an issue which clinical studies indicate is more problematic in mice than humans.^{34,35}

The differences observed between the renal radioactivity concentrations produced by the maleimide- and PODS-based radioimmunoconjugates are intriguing. The coronal and transverse PET images reveal higher radioactivity concentrations in the kidneys of the mice injected with the trio of ^{89}Zr -DFO_{Mal}-SC16-MB1 radioimmunoconjugates compared to ^{89}Zr -DFO_{PODS}-DAR2SC16-MB1 (Figure 2). This observation is backed up by the biodistribution data: the renal

radioactivity concentration produced by ^{89}Zr -DFO_{Mal}-DAR2SC16-MB1 at 120 h p.i. was 4.7 ± 0.5 %ID/g, while that of ^{89}Zr -DFO_{PODS}-DAR2SC16-MB1 was 3.3 ± 0.5 %ID/g at the same time point ($p = 0.002$). A similar trend was seen with the isotype control radioimmunoconjugates. In this case, ^{89}Zr -DFO_{Mal}-DAR2hIgG1-MB1 produced a radioactivity concentration of 6.7 ± 1.1 %ID/g in the kidneys at 120–128 h p.i., while ^{89}Zr -DFO_{PODS}-DAR2hIgG1-MB1 yielded 4.0 ± 0.3 %ID/g at the same time point ($p = 0.002$). This trend among the isotype control radioimmunoconjugates is especially informative, as these two agents are not subject to target-mediated clearance and thus circulate in the blood longer than their DLL3-targeting counterparts. In addition, the kidney-to-blood radioactivity concentration ratios produced by ^{89}Zr -DFO_{PODS}-DAR2SC16-MB1 and ^{89}Zr -DFO_{PODS}-DAR2hIgG1-MB1 were significantly lower than those created by ^{89}Zr -DFO_{Mal}-DAR2SC16-MB1 and ^{89}Zr -DFO_{Mal}-DAR2hIgG1-MB1 (Figure 2).

In an effort to delve further into these differences, a longitudinal PET study was conducted to facilitate a head-to-head comparison of the *in vivo* performance of ^{89}Zr -DFO_{PODS}-DAR2SC16-MB1 and ^{89}Zr -DFO_{Mal}-DAR2SC16-MB1 in mice bearing subcutaneous H82 human SCLC xenografts (Figure 3A). Acute biodistribution data were also

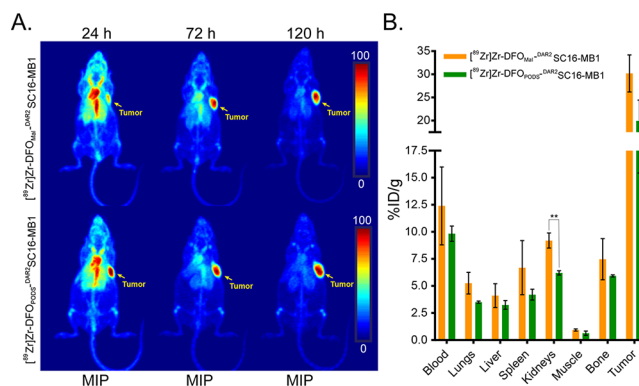


Figure 3. (A) Serial ^{89}Zr -immunoPET MIP images of athymic nude mice bearing DLL3-expressing H82 xenografts acquired at 24, 72, and 120 h p.i. of ~ 230 μCi (1.7 mg/kg) of ^{89}Zr -DFO_{Mal}-DAR2SC16-MB1 and ^{89}Zr -DFO_{PODS}-DAR2SC16-MB1 suspended in 200 μL PBS and injected via the lateral tail vein. Both panels illustrate the gradual accretion of radioactivity in the tumors as well as the slow clearance of the radioimmunoconjugates from the blood. The PET images suggest slightly higher radioactivity concentrations in the blood of the mice injected with the maleimide-based radioimmunoconjugate. (B) *Ex vivo* biodistribution profiles of ^{89}Zr -DFO_{Mal}-DAR2SC16-MB1 and ^{89}Zr -DFO_{PODS}-DAR2SC16-MB1 obtained by harvesting the tissues of the mice in the PET imaging study after the 120 h p.i. scan. ** indicates $p < 0.01$. Tables of the %ID/g values and tumor-to-background radioactivity concentration ratios can be found in Tables S3 and S4.

collected for each of the tumor-bearing mice after the final imaging time point (120 h) (Figure 3B). The PET images for both radioimmunoconjugates revealed the steady accumulation of radioactivity in the DLL3-expressing tumors over the course of the experiment, and no particularly stark differences in the *in vivo* profiles of the two agents were apparent. The *ex vivo* biodistribution analysis performed after the final imaging time point (120 h p.i.) revealed a significant difference between the radioactivity concentrations of ^{89}Zr -DFO_{PODS}-DAR2SC16-

MB1 (6.2 ± 0.2 %ID/g) and [^{89}Zr]Zr-DFO_{Mal}-^{DAR2}SC16-MB1 (9.2 ± 0.7 %ID/g) ($p = 0.01$, Figure 3B) in the kidney, a tissue that has a redox microenvironment conducive for retro-Michael reactions owing to the presence of thiol-rich molecules such as glutathione.³⁶ This $\sim 50\%$ increase in the renal uptake of the maleimide-based probe could be problematic in the context of the immunoPET imaging of lesions in the kidneys, but—even more concerning—it also suggests that toxic payloads conjugated to ADCs via maleimide–thiol linkages may similarly be released in or migrate to the kidneys. Presumably, this sort of *in vivo* decomposition of ADCs could lead to off-target toxicity to the kidneys and other healthy organs.³⁷

CONCLUSIONS

In the end, we believe that the findings of this investigation can be distilled into two points. First, the DAR2 bioconjugation method based on the two-component reduction buffer produced more homogeneous immunoconjugates than strategies that use high or low concentrations of TCEP. Second, a [^{89}Zr]Zr-labeled variant of SC16-MB1 synthesized using the PODS bioconjugation scaffold—*i.e.*, [^{89}Zr]Zr-DFO_{PODS}-^{DAR2}SC16-MB1—yielded lower radioactivity concentrations in the kidneys than an analogous radioimmunoconjugate constructed using a maleimide-bearing bifunctional chelator.

It is important to acknowledge that this work does indeed have its limitations. First, the shift from Mal-DFO to PODS-DFO-Fe is accompanied by a pair of minor complications: (i) Mal-DFO seems to produce more homogeneous immunoconjugates using the DAR2 method, and (ii) the synthesis of DFO-bearing immunoconjugates using PODS-DFO-Fe requires an EDTA washing step that includes the brief exposure of the antibody to pH 4.5 to remove the coordinated Fe. Second, all of the experiments described have been carried out using a single cysteine-engineered antibody platform. Though we are confident that the overarching lessons of this work are generalizable, the application of the bioconjugation strategies we describe would certainly require optimization if used in conjunction with wild-type IgG or other cysteine-engineered antibodies. The microenvironment of cysteine residues may vary from one antibody to another, changes that can lead to variations in the reactivity of these residues during bioconjugation protocols and the interplay between bioconjugation and *in vivo* performance. Along these lines, it is important to note that the differences in *in vivo* performance that we observed in this study between [^{89}Zr]Zr-DFO_{PODS}-^{DAR2}SC16-MB1 and [^{89}Zr]Zr-DFO_{Mal}-^{DAR2}SC16-MB1 were significantly less dramatic than those previously found between PODS- and maleimide-based variants of [^{89}Zr]Zr-DFO-huA33.²³ This underscores that while PODS-based conjugations are consistently beneficial across IgG platforms, the degree to which this alternative approach improves *in vivo* behavior can vary.

These caveats aside, a growing body of evidence suggests that site-specifically modified radioimmunoconjugates synthesized using PODS offer superior *in vivo* performance. In this case, the *in vivo* behavior of [^{89}Zr]Zr-DFO_{PODS}-^{DAR2}SC16-MB1 certainly marks it as a strong candidate for clinical translation. Plans are currently underway to expand the applications of PODS-based bioconjugations and develop second-generation reagents with enhanced selectivity and reactivity.

ASSOCIATED CONTENT

Supporting Information

The Supporting Information is available free of charge at <https://pubs.acs.org/doi/10.1021/acs.bioconjchem.1c00121>.

Experimental procedures, mass spectrometry results, stability assay results, and tables of biodistribution data and tissue-to-blood radioactivity concentration ratios (PDF)

AUTHOR INFORMATION

Corresponding Author

Brian M. Zeglis – Department of Radiology, Memorial Sloan Kettering Cancer Center, New York 10065, United States; Department of Chemistry, Hunter College, City University of New York, New York 10021, United States; Department of Radiology, Weill Cornell Medical College, New York 10021, United States; orcid.org/0000-0002-9091-744X; Phone: 212-896-0433; Email: bz102@hunter.cuny.edu; Fax: 212-772-5332

Authors

Sai Kiran Sharma – Department of Radiology, Memorial Sloan Kettering Cancer Center, New York 10065, United States; Department of Chemistry, Hunter College, City University of New York, New York 10021, United States
Pierre Adumeau – Department of Chemistry, Hunter College, City University of New York, New York 10021, United States
Outi Keinänen – Department of Radiology, Memorial Sloan Kettering Cancer Center, New York 10065, United States; Department of Chemistry, Hunter College, City University of New York, New York 10021, United States
Vikram Sisodiya – Abbvie Stemcentrx, South San Francisco, California 94080, United States
Hetal Sarvaiya – Abbvie Stemcentrx, South San Francisco, California 94080, United States
Robert Tchelepi – Abbvie Stemcentrx, South San Francisco, California 94080, United States
Joshua A Korsen – Department of Pharmacology, Weill Cornell Medical College, New York 10021, United States
Jacob Pourat – Department of Radiology, Memorial Sloan Kettering Cancer Center, New York 10065, United States
Kimberly J. Edwards – Department of Radiology, Memorial Sloan Kettering Cancer Center, New York 10065, United States
Ashwin Ragupathi – Department of Radiology, Memorial Sloan Kettering Cancer Center, New York 10065, United States
Omar Hamdy – Abbvie Stemcentrx, South San Francisco, California 94080, United States
Laura R. Saunders – Abbvie Stemcentrx, South San Francisco, California 94080, United States
Charles M. Rudin – Department of Medicine and Molecular Pharmacology Program, Memorial Sloan Kettering Cancer Center, New York 10065, United States
John T. Poirier – Department of Medicine and Molecular Pharmacology Program, Memorial Sloan Kettering Cancer Center, New York 10065, United States
Jason S. Lewis – Department of Radiology, Molecular Pharmacology Program, and Radiochemistry and Molecular Imaging Probes Core, Memorial Sloan Kettering Cancer Center, New York 10065, United States; Department of Pharmacology and Department of Radiology, Weill Cornell

Medical College, New York 10021, United States;

orcid.org/0000-0001-7065-4534

Complete contact information is available at:

<https://pubs.acs.org/10.1021/acs.bioconjchem.1c00121>

Notes

The authors declare the following competing financial interest(s): H.S. is currently an employee of Abbvie, Inc. V.S., R.T., O.H., and L.R.S. are former employees of Abbvie, Inc. C.M.R. serves on the Scientific Advisory Boards of Bridge Medicines, Earli, and Harpoon Therapeutics.

ACKNOWLEDGMENTS

This work was supported by a grant from the Druckenmiller Center for Lung Cancer Research and the National Institutes of Health: U01CA213359 (JTP & JSL), R01CA213448 (JTP, CMR, & JSL), R01CA240963 (BMZ), U01CA221046 (BMZ & JSL), R01CA204167 (BMZ & JSL), R21EB030275 (BMZ), R01CA244327 (BMZ), and R35CA232130 (JSL). SKS acknowledges support from the Tow Postdoctoral Fellowship Program. The authors also thank the MSKCC Small Animal Imaging Core Facility, the MSKCC Radiochemistry and Molecular Imaging Probe core, the MSKCC Anti-Tumor Assessment Core, and the Tri-Institutional Laboratory of Comparative Pathology, which were supported in part by NIH grant P30 CA08748. Finally, the authors also thank Mr. William H. and Mrs. Alice Goodwin and the Commonwealth Foundation for Cancer Research as well as the MSK Center for Experimental Therapeutics.

ABBREVIATIONS

DLL3, delta-like ligand 3; SCLC, small cell lung cancer; PET, positron emission tomography; DFO, desferrioxamine; PODS, phenyloxadiazolyl methyl sulfone; Mal, maleimide; DAR, DFO-to-antibody ratio; TCEP, tris(2-carboxyethyl) phosphine; ADC, antibody-drug conjugate; TBR, tumor-to-blood ratio

REFERENCES

- (1) Agarwal, P., and Bertozzi, C. R. (2015) Site-specific antibody-drug conjugates: the nexus of bioorthogonal chemistry, protein engineering, and drug development. *Bioconjugate Chem.* 26 (2), 176–92.
- (2) Jain, N., Smith, S. W., Ghone, S., and Tomczuk, B. (2015) Current ADC linker chemistry. *Pharm. Res.* 32 (11), 3526–40.
- (3) Massa, S., Xavier, C., Muyldermans, S., and Devoogdt, N. (2016) Emerging site-specific bioconjugation strategies for radioimmuno-tracer development. *Expert Opin. Drug Delivery* 13 (8), 1149–63.
- (4) Akkapeddi, P., Azizi, S. A., Freedy, A. M., Cal, P., Gois, P. M. P., and Bernardes, G. J. L. (2016) Construction of homogeneous antibody-drug conjugates using site-selective protein chemistry. *Chemical Science* 7 (5), 2954–2963.
- (5) Adumeau, P., Sharma, S. K., Brent, C., and Zeglis, B. M. (2016) Site-specifically labeled immunoconjugates for molecular imaging—part 2: Peptide tags and unnatural amino acids. *Molecular Imaging and Biology* 18 (2), 153–65.
- (6) Adumeau, P., Sharma, S. K., Brent, C., and Zeglis, B. M. (2016) Site-specifically labeled immunoconjugates for molecular imaging—part 1: Cysteine residues and glycans. *Molecular Imaging and Biology* 18 (1), 1–17.
- (7) Junutula, J. R., Raab, H., Clark, S., Bhakta, S., Leipold, D. D., Weir, S., Chen, Y., Simpson, M., Tsai, S. P., Dennis, M. S., Lu, Y., Meng, Y. G., Ng, C., Yang, J., Lee, C. C., Duenas, E., Gorrell, J., Katta, V., Kim, A., McDorman, K., Flagella, K., Venook, R., Ross, S., Spencer,

S. D., Lee Wong, W., Lowman, H. B., Vandlen, R., Sliwkowski, M. X., Scheller, R. H., Polakis, P., and Mallet, W. (2008) Site-specific conjugation of a cytotoxic drug to an antibody improves the therapeutic index. *Nat. Biotechnol.* 26 (8), 925–32.

(8) Behrens, C. R., and Liu, B. (2014) Methods for site-specific drug conjugation to antibodies. *MAbs* 6 (1), 46–53.

(9) Zettlitz, K. A., Waldmann, C. M., Tsai, W. K., Tavare, R., Collins, J., Murphy, J. M., and Wu, A. M. (2019) A dual-modality linker enables site-specific conjugation of antibody fragments for (18)F-immuno-PET and fluorescence imaging. *J. Nucl. Med.* 60 (10), 1467–1473.

(10) Wei, C., Zhang, G., Clark, T., Barletta, F., Tumey, L. N., Rago, B., Hansel, S., and Han, X. (2016) Where did the linker-payload go? A quantitative investigation on the destination of the released linker-payload from an antibody-drug conjugate with a maleimide linker in plasma. *Anal. Chem.* 88 (9), 4979–86.

(11) Szijj, P. A., Bahou, C., and Chudasama, V. (2018) Minireview: Addressing the retro-Michael instability of maleimide bioconjugates. *Drug Discovery Today: Technol.* 30, 27–34.

(12) Renault, K., Fredy, J. W., Renard, P. Y., and Sabot, C. (2018) Covalent modification of biomolecules through maleimide-based labeling strategies. *Bioconjugate Chem.* 29 (8), 2497–2513.

(13) Dong, L., Li, C., Locuson, C., Chen, S., and Qian, M. G. (2018) A two-step immunocapture LC/MS/MS assay for plasma stability and payload migration assessment of cysteine-maleimide-based antibody drug conjugates. *Anal. Chem.* 90 (10), 5989–5994.

(14) Christie, R. J., Fleming, R., Bezabeh, B., Woods, R., Mao, S., Harper, J., Joseph, A., Wang, Q., Xu, Z. Q., Wu, H., Gao, C., and Dimasi, N. (2015) Stabilization of cysteine-linked antibody drug conjugates with N-aryl maleimides. *J. Controlled Release* 220, 660–70.

(15) Ponte, J. F., Sun, X., Yoder, N. C., Fishkin, N., Laleau, R., Coccia, J., Lanieri, L., Bogalhas, M., Wang, L., Wilhelm, S., Widdison, W., Pinkas, J., Keating, T. A., Chari, R., Erickson, H. K., and Lambert, J. M. (2016) Understanding how the stability of the thiol-maleimide linkage impacts the pharmacokinetics of lysine-linked antibody-maytansinoid conjugates. *Bioconjugate Chem.* 27 (7), 1588–1598.

(16) Baldwin, A. D., and Kiick, K. L. (2011) Tunable degradation of maleimide-thiol adducts in reducing environments. *Bioconjugate Chem.* 22 (10), 1946–1953.

(17) Khalili, H., Godwin, A., Choi, J.-w., Lever, R., and Brocchini, S. (2012) Comparative binding of disulfide-bridged PEG-Fabs. *Bioconjugate Chem.* 23 (11), 2262–2277.

(18) Li, J., Wang, X. H., Wang, X. M., and Chen, Z. L. (2006) Site-specific conjugation of bifunctional chelator BAT to mouse IgG(1) Fab' fragment. *Acta Pharmacol. Sin.* 27 (2), 237–241.

(19) Badescu, G., Bryant, P., Bird, M., Henseleit, K., Swierkosz, J., Parekh, V., Tommasi, R., Pawlisz, E., Jurlewicz, K., Farys, M., Camper, N., Sheng, X., Fisher, M., Grygorash, R., Kyle, A., Abhilash, A., Frigerio, M., Edwards, J., and Godwin, A. (2014) Bridging disulfides for stable and defined antibody drug conjugates. *Bioconjugate Chem.* 25 (6), 1124–1136.

(20) Morais, M., Nunes, J. P. M., Karu, K., Forte, N., Benni, I., Smith, M. E. B., Caddick, S., Chudasama, V., and Baker, J. R. (2017) Optimisation of the dibromomaleimide (DBM) platform for native antibody conjugation by accelerated post-conjugation hydrolysis. *Org. Biomol. Chem.* 15 (14), 2947–2952.

(21) Smith, M. E. B., Schumacher, F. F., Ryan, C. P., Tedaldi, L. M., Papaioannou, D., Waksman, G., Caddick, S., and Baker, J. R. (2010) Protein modification, bioconjugation, and disulfide bridging using bromomaleimides. *J. Am. Chem. Soc.* 132, 1960–1965.

(22) Fontaine, S. D., Reid, R., Robinson, L., Ashley, G. W., and Santi, D. V. (2015) Long-term stabilization of maleimide-thiol conjugates. *Bioconjugate Chem.* 26 (1), 145–152.

(23) Adumeau, P., Davydova, M., and Zeglis, B. M. (2018) Thiol-reactive bifunctional chelators for the creation of site-selectively modified radioimmunoconjugates with improved stability. *Bioconjugate Chem.* 29 (4), 1364–1372.

(24) Khozeimeh Sarbisheh, E., Dewaele-Le Roi, G., Shannon, W. E., Tan, S., Xu, Y., Zeglis, B. M., and Price, E. W. (2020) DiPODS: A

reagent for site-specific bioconjugation via the irreversible rebridging of disulfide linkages. *Bioconjugate Chem.* 31, 2789.

(25) Davydova, M., Dewaele-Le Roi, G., Adumeau, P., and Zeglis, B. M. (2019) Synthesis and bioconjugation of thiol-reactive reagents for the creation of site-selectively modified immunoconjugates. *J. Visualized Exp.* 145, No. e59063.

(26) Patterson, J. T., Asano, S., Li, X., Rader, C., and Barbas, C. F. (2014) III, Improving the serum stability of site-specific antibody conjugates with sulfone linkers. *Bioconjugate Chem.* 25 (8), 1402–1407.

(27) Toda, N., Asano, S., and Barbas, C. F. (2013) III, Rapid, stable, chemoselective labeling of thiols with Julia-Kocienski-like reagents: A serum-stable alternative to maleimide-based protein conjugation. *Angew. Chem., Int. Ed.* 52 (48), 12592–12596.

(28) Sharma, S. K., Pourat, J., Abdel-Atti, D., Carlin, S. D., Piersigilli, A., Bankovich, A. J., Gardner, E. E., Hamdy, O., Isse, K., Bheddah, S., Sandoval, J., Cunanan, K. M., Johansen, E. B., Allaj, V., Sisodiya, V., Liu, D., Zeglis, B. M., Rudin, C. M., Dylla, S. J., Poirier, J. T., and Lewis, J. S. (2017) Noninvasive interrogation of DLL3 expression in metastatic small cell lung cancer. *Cancer Res.* 77 (14), 3931–3941.

(29) Saunders, L. R., Bankovich, A. J., Anderson, W. C., Aujay, M. A., Bheddah, S., Black, K., Desai, R., Escarpe, P. A., Hampl, J., Laysang, A., Liu, D., Lopez-Molina, J., Milton, M., Park, A., Pysz, M. A., Shao, H., Slingerland, B., Torgov, M., Williams, S. A., Foord, O., Howard, P., Jassem, J., Badzio, A., Czapiewski, P., Harpole, D. H., Dowlati, A., Massion, P. P., Travis, W. D., Pietanza, M. C., Poirier, J. T., Rudin, C. M., Stull, R. A., and Dylla, S. J. (2015) A DLL3-targeted antibody-drug conjugate eradicates high-grade pulmonary neuroendocrine tumor-initiating cells in vivo. *Sci. Transl. Med.* 7 (302), 302ra136.

(30) Spino, M., Kurz, S. C., Chiriboga, L., Serrano, J., Zeck, B., Sen, N., Patel, S., Shen, G., Vasudevaraja, V., Tsirigos, A., Suryadevara, C. M., Frenster, J. D., Tateishi, K., Wakimoto, H., Jain, R., Riina, H. A., Nicolaides, T. P., Sulman, E. P., Cahill, D. P., Golfinos, J. G., Isse, K., Saunders, L. R., Zagzag, D., Placantonakis, D. G., Snuderl, M., and Chi, A. S. (2019) Cell surface notch ligand DLL3 is a therapeutic target in isocitrate dehydrogenase-mutant glioma. *Clin. Cancer Res.* 25 (4), 1261–1271.

(31) Price, E. W., and Orvig, C. (2014) Matching chelators to radiometals for radiopharmaceuticals. *Chem. Soc. Rev.* 43 (1), 260–290.

(32) Liu, H., Chumsae, C., Gaza-Bulseco, G., Hurkmans, K., and Radziejewski, C. H. (2010) Ranking the susceptibility of disulfide bonds in human IgG1 antibodies by reduction, differential alkylation, and LC-MS analysis. *Anal. Chem.* 82 (12), 5219–26.

(33) Tsumoto, K., Umetsu, M., Kumagai, I., Ejima, D., Philo, J. S., and Arakawa, T. (2004) Role of arginine in protein refolding, solubilization, and purification. *Biotechnol. Prog.* 20 (5), 1301–8.

(34) Chomet, M., Schreurs, M., Bolijn, M. J., Verlaan, M., Beaino, W., Brown, K., Poot, A. J., Windhorst, A. D., Gill, H., Marik, J., Williams, S., Cowell, J., Gasser, G., Mindt, T. L., van Dongen, G., and Vugts, D. J. (2020) Head-to-head comparison of DFO* and DFO chelators: selection of the best candidate for clinical ⁸⁹Zr-immunoPET. *Eur. J. Nucl. Med. Mol. Imaging*, 1 DOI: 10.1007/s00259-020-05002-7.

(35) Holland, J. P., Divilov, V., Bander, N. H., Smith-Jones, P. M., Larson, S. M., and Lewis, J. S. (2010) ⁸⁹Zr-DFO-J591 for immunoPET of prostate-specific membrane antigen expression in vivo. *J. Nucl. Med.* 51 (8), 1293–300.

(36) Lash, L. H. (2005) Role of glutathione transport processes in kidney function. *Toxicol. Appl. Pharmacol.* 204 (3), 329–42.

(37) Drake, P. M., and Rabuka, D. (2017) Recent Developments in ADC Technology: Preclinical Studies Signal Future Clinical Trends. *BioDrugs* 31 (6), 521–531.